

# Current-Limiting Properties of a Hybrid Superconducting Flux-Offset-Type FCL

Sang-Yong Park<sup>1</sup> · Hye-Won Choi<sup>1</sup> · In-Sung Jeong<sup>1</sup> · Hyo-Sang Choi<sup>1</sup>

Received: 21 March 2017 / Accepted: 17 April 2017 / Published online: 28 April 2017  
© Springer Science+Business Media New York 2017

**Abstract** The global consumption of electricity is on the rise due to the industrial and population growth. The number of power generation and distribution facilities is increasing in order to meet the growing demand. Furthermore, the low impedance of power systems is causing a fault current that exceeds the capacity of the existing circuit breaker. In this paper, a method was suggested which limits the initial fault current by combining a superconducting fault current limiter (SFCL) with the existing flux-offset-type fault current limiter (FCL). Results showed that the initial fault current within a half cycle was limited by approximately 60%, while the fault current after a half cycle was limited by approximately 80%. Overall, 99.8% of the fault current was limited, while the power burden on the SFCL was reduced by more than 50%.

**Keywords** Flux-offset-type fault current limiter (FCL) · Initial fault current · Hybrid superconducting flux-offset-type fault current limiter (SFO-FCL) · Superconducting fault current limiter (SFCL)

## 1 Introduction

Many countries use a loop system in their power supply system, so that if the power transmission in one part becomes unworkable, it can immediately supply power to another part. However, a high initial fault current can induce a fault in a system. It is estimated by the breaking capacity of a current limiter or circuit breaker based on the initial fault current. The swift limiting of the initial fault current may not only reduce the rupturing capacity of a current limiter or circuit breaker, but it can also protect the connected devices. Failure to immediately limit this high initial fault current will give rise to the breakdown of the power devices connected to the system or shortened durability, thereby resulting in economic loss [1]. As a solution, a method was suggested which limits the initial fault current by combining the superconducting fault current limiter (SFCL) with the existing flux-offset-type fault current limiter (FCL)

The SFCL used all carried power consumption and swiftly limited the fault current. The power consumption is power consumed per unit hour. Therefore, if the time for limiting the fault current is longer, the power consumption is higher. The SFCL would be perilous about the breakdown in case it takes responsibility for all power burdens [2, 3].

The flux-offset-type FCL is made up of current transformer (CT), switching control system, and vacuum interrupter. The flux-offset-type FCL effectively limits the fault current after a half cycle by using the impedance for the occurred inductive reactance based on the principles of a transformer. However, it operates only after a half cycle [4, 5]. The fault current before the limit damages the connected device to the loop system and the flux-offset-type FCL. The current limiter and circuit breaker have to respond to a very serious fault current in a fault condition. The current limiter and circuit breaker have to respond to the fault current

---

✉ Hyo-Sang Choi  
hyosang@chosun.ac.kr

Sang-Yong Park  
sangyong4400@gmail.com

Hye-Won Choi  
vjvldnjs@naver.com

In-Sung Jeong  
no21park@hanmail.net

<sup>1</sup> Department of Electrical Engineering, Chosun University,  
309 Pilmun-daero, Gwangju 61452, Korea

in fault condition. Therefore, this paper suggested a hybrid superconducting flux-offset-type FCL (SFO-SFCL) which uses the impedance of the flux-offset-type FCL and adds the SFCL to its secondary winding for the reduced power burden of the SFCL.

### 1.1 Operating Mechanism of a Flux-Offset-Type FCL

#### 1.2 During a Normal Operation

The transformer of the flux-offset-type FCL requires windings, so that the primary and secondary coils have the same inductance as shown in (1) [5, 7]. According to Ampere’s law the normal current that flows in the primary coil of the transformer induces the primary flux. This primary flux flows through the iron core toward the secondary coil, thereby inducing a current in the closed secondary coil of the transformer, as stated in Faraday’s law of electromagnetic induction. This is called the secondary induced current. Equation (2) shows Neumann-Kopp’s law, which expressed Faraday’s law of electromagnetic induction as a formula.

$$a = \frac{N_1}{N_2} = \frac{E_1}{E_2} = \frac{l_2}{l_1} \tag{1}$$

$$e = -N \frac{d\phi}{dt} [V] \tag{2}$$

The force that creates a secondary induced current is called induced electromotive force. The effective value of the induced electromotive force, according to the flux, is shown in equations (3) and (4). The induced electromotive force is proportional to the variation of the primary flux over time. It can also have a negative value, which means that the secondary induced current caused by the induced electromotive force flows in the direction that offsets the variation of the primary flux.

$$e_1 = 4.44 \cdot f \cdot N_1 \cdot \phi_m [V] \tag{3}$$

$$e_2 = 4.44 \cdot f \cdot N_2 \cdot \phi_m [V] \tag{4}$$

The offset of the primary and secondary flux is expressed in an equation on obtaining an inductance, as shown in (5).

$$L = \frac{N \bullet \phi}{I} [H] \tag{5}$$

Using (6) and (7), the figure of impedance is 0 Ω for the inductive reactance. Therefore, the flux-offset-type transformer allows a normal current flow without any loss during a normal operation.

$$L = L_1 + L_2 = \frac{N_1 \phi_1}{I_1} + (-\frac{N_2 \phi_2}{I_2}) = 0[H] \tag{6}$$

$$X_L = \omega \cdot L = 2\pi \cdot f \cdot L = 2\pi \cdot f \cdot 0 = 0[\Omega] \tag{7}$$

#### 1.3 During a Fault Operation

The fault current that flows in the primary coil and the impedance that interrupts the primary current occurred concurrently, because the counter electromotive force occurred by the magnetic induction.

This is called inductive reactance. When the current flowing through the inductance of the primary coil experiences a sudden change, the highest magnetically induced voltage occurs at the inductance, and its magnitude is identical to the maximum source voltage at that moment. The fault current flows through the primary coil of the transformer, thereby inducing a primary flux. By opening the closed secondary circuit when a fault occurs, the secondary coil of the transformer in a normal system does not experience an induced voltage. Since the secondary induced current that offsets the primary flux does not occur, the primary flux flows along the iron core of the transformer. As a result, the impedance, which limits the fault current, can be estimated through (8) and (9). The CT detects the fault current and transfers a signal to the switching control system at the same time. The switching control system will open the b-contact of the vacuum interrupter, and then the high impedance occurs artificially and limits the fault current.

$$L = \frac{N \cdot \phi_1}{I_1} [\Omega] \tag{8}$$

$$X_L = 2\pi \cdot f \cdot L_1 [\Omega] \tag{9}$$

**Table 1** The parameter of a transformer by using the PSCAD/EMTDC

Source impedance type	R-R//L	Winding no. 2 voltage (RMS)	141.4 (V)
Transformer MVA	30 (kVA)	Hysteresis	Basic
Base operation frequency	60 (Hz)	Air core reactance	0.109923 (pu)
Leakage reactance	0.109923 (pu)	Magnetizing current	0.7 (%)
Eddy current losses	0.0009 (pu)	Knee voltage	1.25 (pu)
Copper losses	0.004125 (pu)	Remanent flux	0.0 (H)
Winding no. 1 voltage (RMS)	141.4 (V)	Loop width	14.5 (cm)

### 1.4 PSCAD/EMTDC Simulation Analysis

### 1.5 Hybrid Superconducting Flux-Offset-Type FCL Modeling

The simulation data were analyzed by the PSCAD/EMTDC software program. A flux-offset-type FCL model was constructed using this program, and then it was analyzed with the SFCL.

Table 1 shows the transformer specifications collected from domestic A corporation. It applied the transformer parameter value of the PSCAD/EMTDC.

This simulation designed a quench operation of the SFCL based on previous studies [2–7]. The maximum quenching resistance was  $R_m$ . The transition time was  $t$ . The time constant determining the transition characteristics of the quench was  $T_{sc}$ . The critical current was 0.05 kA.  $R_m$  was 10  $\Omega$ .  $t$  which is rating time of SFCL was 2 ms. The  $T_{sc}$  was 0.25 ms for obtaining 10  $\Omega$  of the  $R_m$  within 2 ms. The quench characteristics designed based on the (10). The b-contact operation speed of the flux-offset-type FCL was 9 ms based on the previous studies [4, 6].

$$S_{SFCL}(t) = R_m(1 - \exp(-t/T_{sc}))[\Omega] \tag{10}$$

### 1.6 Simulation Analysis Results

The simulation model consists of a single power module, a line resistance of 1.0  $\Omega$ , a load, a fault generator, the SFCL, and the b-contact of the vacuum interrupter. The rated normal current was 2 A, which was considered as the voltage of the power supply, line resistance, transformer, and load.

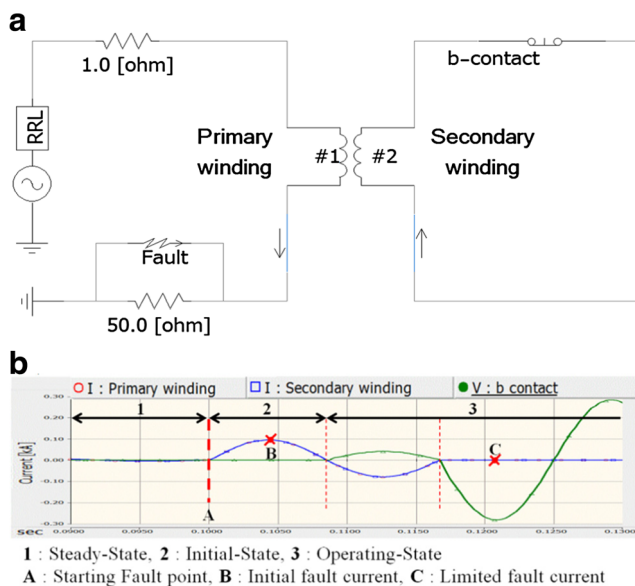


**Fig. 1** Flux-offset-type FCL **a** equivalent circuit diagram, **b** fault-current-limiting characteristics graph

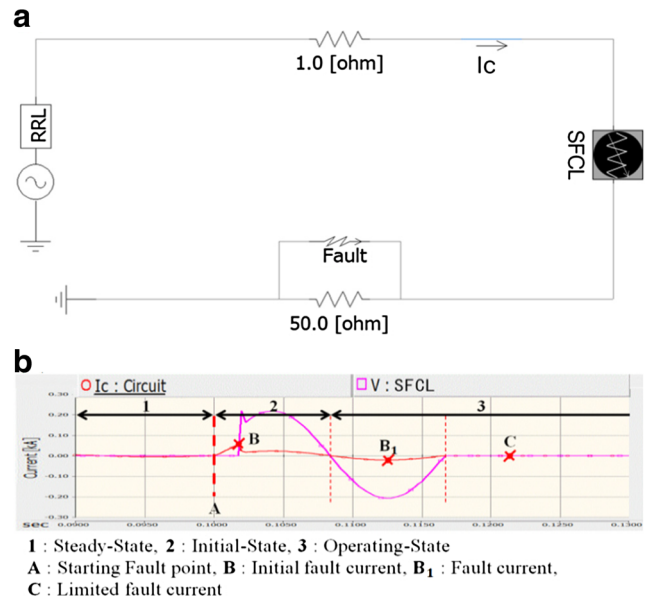


**Fig. 2** SFCL **a** equivalent circuit diagram **b** fault-current-limiting characteristics graph

The fault occurred at 59 ms, and the quench operation of the SFCL started at 2 ms after the fault occurred. The b-contact opening of the flux-offset-type FCL started at 8 ms after the fault occurred. The current within the 0.5 cycle after the fault was interpreted as the initial fault current, while the current after the 0.5 cycle was interpreted as the fault current.

Figure 1a shows the equivalent circuit diagram of the previously suggested flux-offset-type FCL. Figure 1b shows

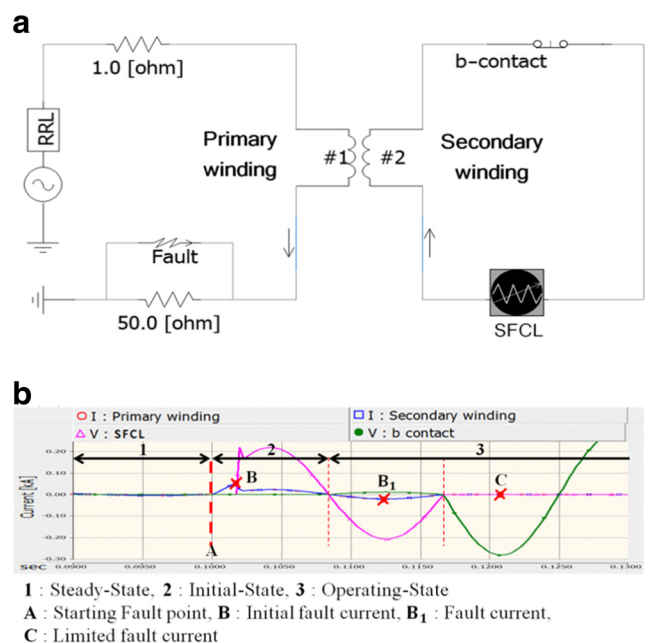


**Fig. 3** Hybrid SFO-FCL **a** equivalent circuit diagram **b** fault-current-limiting characteristics graph

**Table 2** The simulation result of PSCAD/EMTDC

	Flux-offset-type FCL	SFCL	Hybrid SFO-FCL
Initial fault current (A)	93.9	53.6	53.6
Limiting rate of the initial fault current (%)	0	43.1	43.1
Fault current (A)	0.2	21.7	0.2
Limiting rate of the fault current (%)	99.8	76.7	99.8

the fault-current-limiting characteristics graph of the flux-offset-type FCL. The initial fault current was 93.9 A. After 1 cycle, the b-contact was completely opened and the fault current was limited to 0.2 A.

Figure 2a shows the equivalent circuit diagram of the SFCL. Figure 2b shows the fault-current-limiting characteristics graph of the SFCL. Simulation results showed that the initial fault current was reduced from 93.9 to 53.6 A due to the quench of the SFCL. The fault current was decreased from 53.6 to 21.7 A. The limiting rate can be calculated through (11).

$$\left[ \frac{(\text{Initial value} - \text{Result value})}{\text{Initial value}} \times 100 \right] \quad (11)$$

Figure 3a shows the equivalent circuit diagram of the hybrid SFO-FCL. Figure 3b shows the fault-current-limiting characteristics graph of the hybrid SFO-FCL.

In consequence, the initial fault current was limited to 53.6 and 30.4 A after the 0.5 cycle via the SFCL. After 1 cycle, the fault current was limited to 0.2 A. Table 2 shows simulation result of PSCAD/EMTDC.

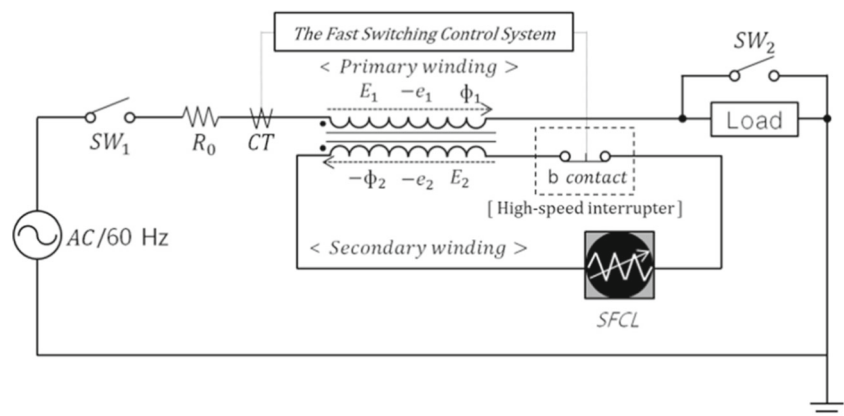
## 2 Experiment

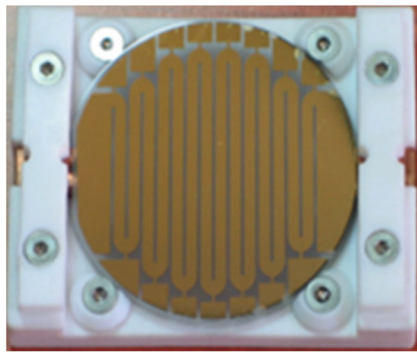
### 2.1 Experimental Process of the Hybrid SFO-FCL

Figure 4 shows the test circuit diagram of the flux-offset-type FCL, which was previously proposed.  $SW_1$  was the

power supply switch,  $SW_2$  was the fault generation switch, and  $R_0$  was the line resistance. In order to detect the fault current, a CT was connected to the primary winding of the transformer. The b-contact was a mechanical switch. Furthermore, this research team developed and used a high-speed interrupter, which receives signals from the CT upon the occurrence of a fault in order to conduct switching. The applied voltage was 200 V, and the turn ratio of the primary-to-secondary coil in the transformer was 4:4. A 50- $\Omega$  load was connected to the primary winding of the transformer, and a high-speed interrupter was used for the secondary winding to form a short circuit. When power was applied by  $SW_1$ , the two fluxes from the primary and secondary coils were mutually offset in the normal condition, as shown in (8). Accordingly, there was no reactor inductance and the line impedance was 0  $\Omega$ , as shown in (8).

$SW_2$  was the fault generation switch. In this test, a line-to-ground fault was conducted because of its common. When a line-to-ground fault was generated by the  $SW_2$ , the CT detected the fault current, and the high-speed control switching system applied power to the high-speed interrupter. When power was applied, the b-contact of the high-speed interrupter was turned off, thus opening the secondary short circuit of the transformer. Accordingly, it was not offset by the fluxes of the primary and secondary coils of the transformer. As shown in (8) and (9), the  $\Phi_1$  of the primary coil of the transformer created a reactor inductance by generating a certain impedance. As a total impedance on the line, a certain reactance value was determined, as shown in (11). This impedance limits the fault current.

**Fig. 4** The experiment equivalent circuit of the hybrid SFO-FCL



**Fig. 5** The resistive SFCL design

A circuit with the same conditions as the simulation was organized for an actual experiment. The SFCL used was the resistive YBCO thin-film type. This structure was simple and easy to apply to various modules.

Figure 5 was a resistive SFCL design was used in the experiments. Specifications of the SFCL showed a diameter of 2 in, width of 2 mm, total length of 540 mm, YBCO layer thickness of 0.3 mm, and Au layer thickness of 0.1 ~ 0.2 mm [1, 2]. A high-speed interrupter was used for the b-contact of the flux-offset-type FCL in order to ensure a prompt and accurate opening operation [5].

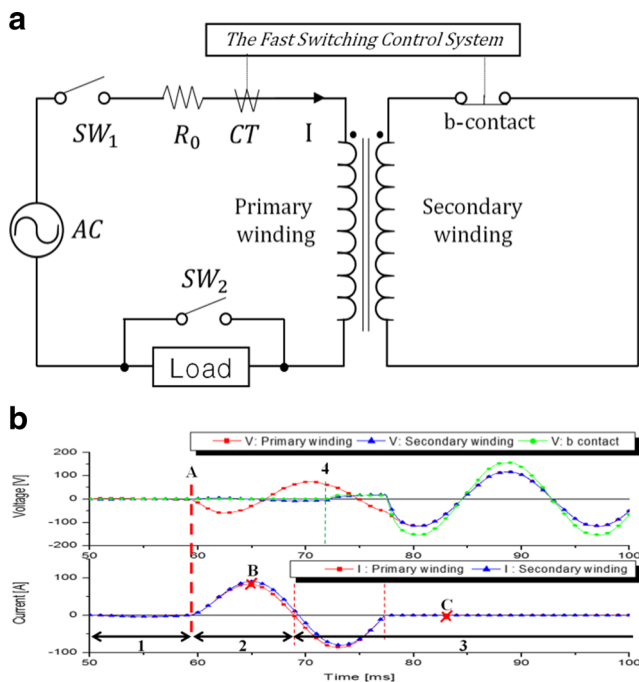


**Fig. 6** Flux-offset-type FCL **a** equivalent circuit diagram for the experiment, **b** fault-current-limiting characteristics graph of the experiment

## 2.2 Experiment Results

In the same way as the simulation analysis, it was interpreted as the initial fault current when the current was within a 0.5 cycle after the fault occurrence, while the current after a 0.5 cycle was interpreted as the fault current. The fault occurred at 59 ms, and the quench of the superconducting current limiter started at approximately 62 ms (after the fault occurred at approximately 3 ms). The b-contact opening of the flux-offset-type FCL started at approximately 72 ms (after the fault occurred at approximately 13 ms). It showed a difference between the simulation and experiment, wherein the b-contact opening of the flux-offset-type FCL of the simulation started at 8 ms after the fault occurred, while that of the experiment started at 13 ms. For these reasons, it took 1.8 ms of the time for CT to detect the fault current and revitalize the solenoid valve (SV) that would operate the vacuum interrupter (VI) after the fault occurred. The VI started to operate at 3.2 ms, wherein the current applied to the SV has reached its maximum value [6].

Figure 6a shows the experimental circuit diagram of the previously suggested flux-offset-type FCL. Figure 6b shows the fault-current-limiting characteristics graph of the flux-offset-type FCL. The results of the experiment showed that the initial fault current was 83.3 A, and it was not limited. After 1 cycle, the fault current was limited to 0.1 A, as the b-contact was completely opened.

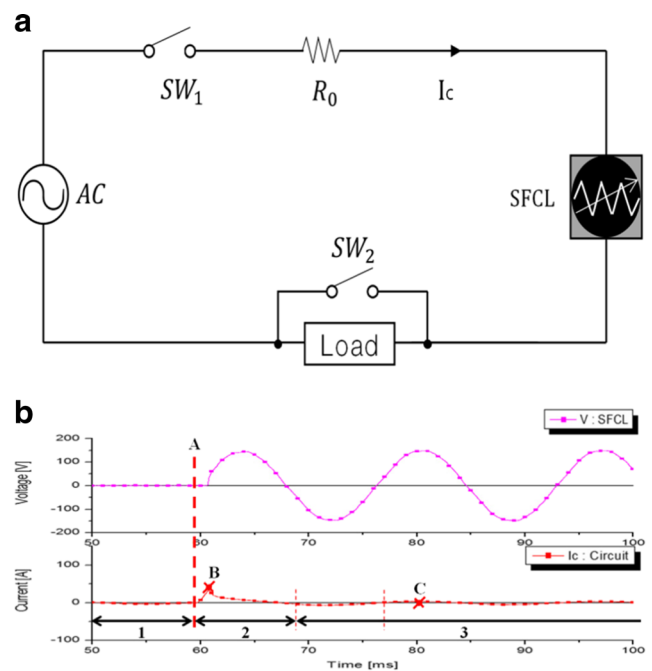


**Fig. 7** SFCL **a** equivalent circuit diagram for the experiment, **b** fault-current-limiting characteristics graph of the experiment

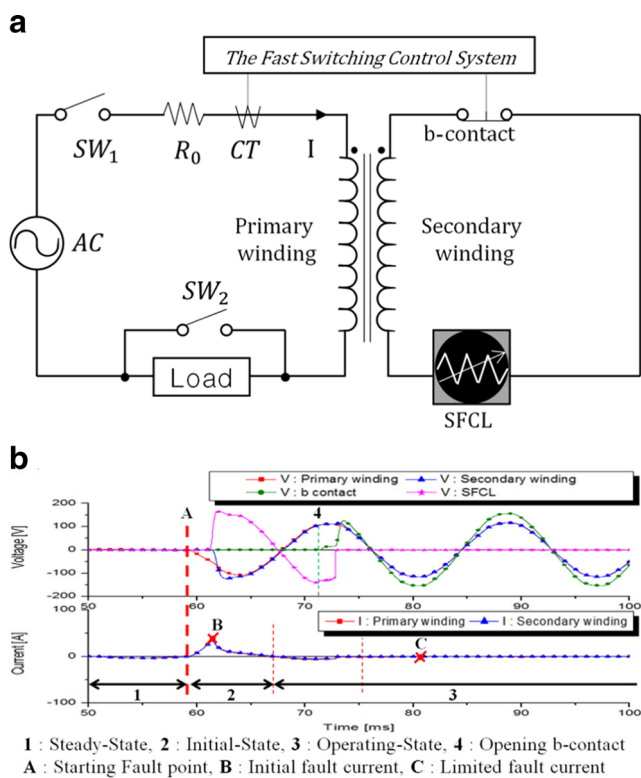


**Fig. 8** Hybrid SFO-FCL **a** equivalent circuit diagram for the experiment **b** fault-current-limiting characteristics graph of the experiment

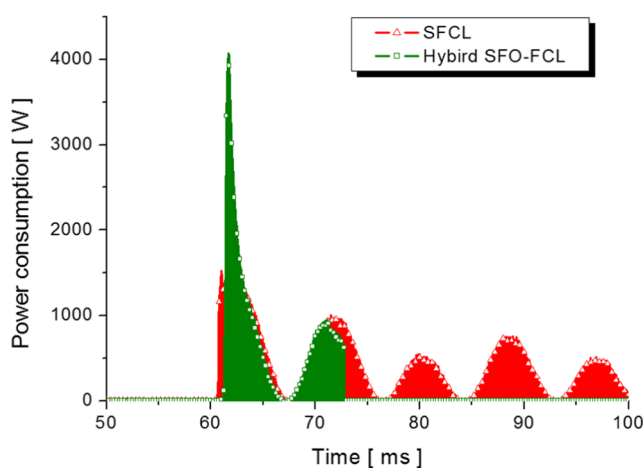
Figure 7a shows the experimental circuit diagram of the previously suggested the SFCL. Figure 7b shows the fault-current-limiting characteristics graph of the SFCL. The experiment was conducted in order to investigate the fault-current-limiting characteristics of the SFCL that was used in this study. Results showed that the initial fault current was reduced to 33.3 A due to the quench of the SFCL. The fault current was limited to 3.2 A.

Figure 8a shows the equivalent circuit diagram for the experiment on the hybrid SFO-FCL. The SFCL was combined with the secondary part of the existing flux-offset-type FCL.

Figure 8b shows the fault-current-limiting characteristics graph of the hybrid SFO-FCL. In result, the initial fault current was reduced to 33.2 A due to the quench of the SFCL.

**Table 3** Simulation result of the experiment

	Flux-offset-type FCL	SFCL	Hybrid SFO-FCL
Initial fault current (A)	83.3	33.3	33.3
Limiting rate of the initial fault current (%)	0	60	60
Fault current (A)	0.1	3.2	0.1
Limiting rate of the fault current (%)	99.8	96.1	99.8



**Fig. 9** Comparison power consumption characteristics of the SFCL and the hybrid SFO-FCL

The fault current was limited to 3.2 A. After approximately 2 ms, the fault current was limited to 0.1 A due to the complete opening.

The initial-fault-current-limiting rate of the simulation was 42.9%, while that of the experiment was 60%. The reason is the existence of the impedance of the external factors and specific resistivity of the used machine in the experiment (Table 3).

### 2.3 Comparison and Analysis of the Power Burdens of the SFCL

Figure 9 shows a graph that compares the power consumption characteristics when the SFCL was operated in the single and hybrid system. Figure 7b shows the fault-current-limiting characteristics of the SFCL, and Fig. 8b shows the fault-current-limiting characteristics of the hybrid SFO-FCL. These were compared and analyzed in order to determine how much the power burden was reduced. The power burden on the SFCL was estimated by multiplying the voltage (V), which is the energy per unit time and the current (A) with integral calculus. The fault occurred at approximately 59 ms.

According to the Fig. 7, the power consumption of the SFCL was 28,168.07 W and that of the SFCL used in the hybrid SFO-FCL was lower by half with 11,951.38 W.

### 3 Conclusions

The initial fault current may give rise to a failure of the devices connected to a current limiter and circuit breaker. Therefore, the rupturing capacity of a current limiter or circuit breaker is estimated based on the initial fault current. An immediate limiting of the initial fault current may not only reduce the rupturing capacity of a current limiter or circuit breaker, but it can also protect the connected devices.

This paper was suggested a method which limits the initial fault current by combining the SFCL with the existing FCL. Three variations, the flux-offset-type FCL, the SFCL, the hybrid SFO-SFCL, have applied before conducting the comparative experiments. The initial-fault-current-limiting rates of the SFCL and the hybrid SFO-FCL were higher than that of the flux-offset-type FCL by 60% due to the restriction that the SFCL has on the initial fault current. In addition, the power burden of the hybrid SFO-SFCL is the lowest in the experiment.

Therefore, the hybrid SFO-FCL was suited to achieve high initial-fault-current-limiting rate and reduce the power burden of the SFCL. Economic benefits can be obtained by using a minimal SFCL. The hybrid SFO-FCL can also be applied to real power systems through continued research.

**Acknowledgments** This study was supported by research fund from Chosun University, 2016.

### References

1. Choi, H.S., Hyun, O.B., Kim, H.R., Park, K.B.: Switching properties of a hybrid type superconducting fault current limiter using YBCO stripes. *IEEE Trans. Appl. Supercond.* **14**(3), 1833–1838 (2002)
2. Kim, H.R., Hyun, O.H., Choi, H.S., Cha, S.D., Oh, J.M.: Resistance development in superconducting fault current limiters prior to quench completion. *IEEE Trans. Appl. Supercond.* **13**(2), 2032–2035 (2003)
3. Lim, S.H., Lee, S.R., Choi, H.S., Han, B.S.: Analysis of operational characteristics of flux-lock type SFCL combined with power compensator. *IEEE Trans. Appl. Supercond.* **15**(2), 2043–2046 (2005)
4. Choi, H.S., Jung, B.I., Cho, Y.S.: Transient characteristics of a flux-coupling type superconducting fault current limiter according to winding direction. *IEEE Trans. Appl. Supercond.* **19**(3), 1827–1830 (2009)
5. Choi, H.W., Jung, B.I., Choi, H.S.: Analysis of the operation characteristics of the flux offset-type fault current limiter for reinforcing the safety of an electric system. *J. Supercond. Novel Magn.* **28**(2), 645–649 (2015)
6. Jung, B.I., Choi, H.S.: Operational characteristics of the FCL using the mechanical contact in the power system. *KIEE* **65**(5), 878–882 (2016)
7. Jung, B.I., Choi, H.S.: Characteristics of the magnetic flux-offset type FCL by switching component. *Progress Supercond. Cryogenics* **18**(2), 18–20 (2016)